Letter

Existence of corner modes in elastic twisted kagome lattices

Hrishikesh Danawe,[1] Heqiu Li,[2] Hasan Al Ba'ba'a,[1] and Serife Tol[1,*]
[1]*Department of Mechanical Engineering, University of Michigan, Ann Arbor, Michigan 48109-2125, USA*
[2]*Department of Physics, University of Michigan, Ann Arbor, Michigan 48109-2125, USA*

(Received 15 July 2021; revised 1 November 2021; accepted 17 November 2021; published 20 December 2021)

This Letter investigates the emergence of corner modes in elastic twisted kagome lattices at a critical twist angle, known as the self-dual point. We show that special types of corner modes exist and they are localized at very specific types of corners independent of the overall shape of the finite lattice. Moreover, these modes appear even in the perturbed lattice at the corners with mirror planes. By exploring their counterparts in electronic systems, we attribute such corner modes to charge accumulation at the boundary, which is confirmed by the plot of charge distribution in a finite lattice.

DOI: 10.1103/PhysRevB.104.L241107

In the early 1990s, by drawing an analogy to the quantum theory of solids, it was theoretically and experimentally shown that acoustoelastic waves propagating through a periodic array of scatterers exhibit frequency regimes in which the waves cannot propagate [1–3], analogous to the electronic band gaps in semiconductors [4–7]. Since then, the study of periodically engineered artificial materials (also referred to as phononic crystals and metamaterials) has matured into an exciting research field. The band gaps and dispersive properties of phononic crystals and metamaterials [8–10] have resulted in unconventional approaches in various applications including sound and vibration attenuation [11,12], cloaking [13], lensing [14,15], subwavelength imaging [16], and energy harvesting [17].

In recent years, the discovery of topological insulators in electronic systems has led to the study of the topological phases of phononic crystals, inspired by their counterparts in photonic systems [18]. A mechanical system is said to be *topological* or *topologically protected* when certain conditions and symmetries are present in the dynamical system. For instance, topological edge states observed in acoustic [19] and elastic [20] kagome lattices are attributed to the preserved C_3 symmetry in the lattice structure after the degeneracy at the Dirac cone at the K point is lifted (a further discussion on the symmetry types in mechanical metamaterials can be found in Ref. [21]). The growing research interest in the topological phases in mechanical systems stems from their special wave properties that offer immunity against defects and imperfections, no wave backscattering, as well as unidirectional wave transmission [18,22]. Originally introduced in electronic/quantum systems, various types of topological states in mechanical systems have been studied. These include the quantum Hall effect [23–25], the quantum spin Hall effect [26–28], the quantum valley Hall effect [20,28–31], Majorana edge states [32], edge states in polyatomic lattices [33], and topological pumping in quasiperiodic systems [34,35]. More recently, higher-order topological insulators have been discovered, offering the unique ability to exhibit in-gap $(d-2)$-dimensional modes [36–38], which goes beyond regular $(d-1)$-dimensional edge states in other topological systems, where d is the dimension of the space.

This effort is particularly focused on the emergence of corner modes in a class of twisted kagome lattices with in-plane motion. The considered twisted kagome lattice is an example of Maxwell lattices, which have been at the heart of recent developments in the field of topological mechanics [39–42]. The configuration of the kagome lattice is shown in Fig. 1(a), which is inspired from a recent study by Fruchart *et al.* [43]. A unit cell or lattice is characterized by three discrete equal masses m, each of which moves in plane in the x and y directions, making a total of six degrees of freedom per unit cell. The masses at the lattice sites are interconnected via central force bonds of stiffness k, and its shape is controlled by a twist angle θ, with perfect hinges at the nodes. As such, the unit cell dynamics exhibit a very interesting property, referred to as *duality*, which means that two different configurations (or twist angles) can exhibit identical dispersion relations [43]. The duality occurs about a critical angle $\theta_c = \pi/4$; hence, a lattice with twist angles $\theta_c \pm \delta\theta$ exhibits an identical dispersion relation. Such a critical point is referred to as a *self-dual point*. The dispersion relation of a self-dual kagome lattice ($\theta = \theta_c$) has three distinct degenerate dispersion bands with two identical copies of dispersion branches on top of each other, as shown in Fig. 1(b), computed by calculating the eigenfrequencies ω of the unit cell's dynamical matrix at selected values of a wave vector $\mathbf{k} = \{k_x, k_y\}$. See the Supplemental Material (SM) [44] for calculation details (see also Refs. [43,45] therein). The static and dynamic behaviors of elastic twisted kagome lattices are well studied in literature. Hutchinson and Fleck [46] investigated the collapse mechanisms (also known as floppy modes) of regular kagome and strain-producing mechanisms in twisted kagome lattices. Later, Sun *et al.* [47] studied the bulk and surface zero-frequency floppy modes of regular and twisted kagome lattices under different boundary conditions. Later, Rocklin *et al.* [48] demonstrated the topological

*Corresponding author: stol@umich.edu

 ©2021 American Physical Society

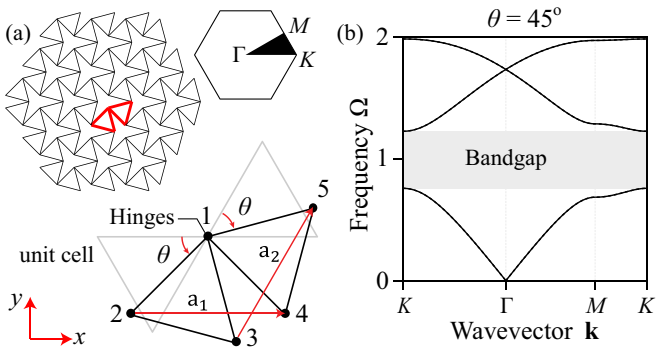

FIG. 1. (a) A finite structure of a twisted kagome lattice and its unit cell definition. The first irreducible Brillouin zone ($\Gamma - M - K - \Gamma$) is depicted for reference. (b) Dispersion band diagram of a self-dual kagome lattice (i.e., for $\theta = pi/4$) depicting three doubly degenerate dispersion branches. Note that $\Omega = \omega\sqrt{\frac{m}{k}}$.

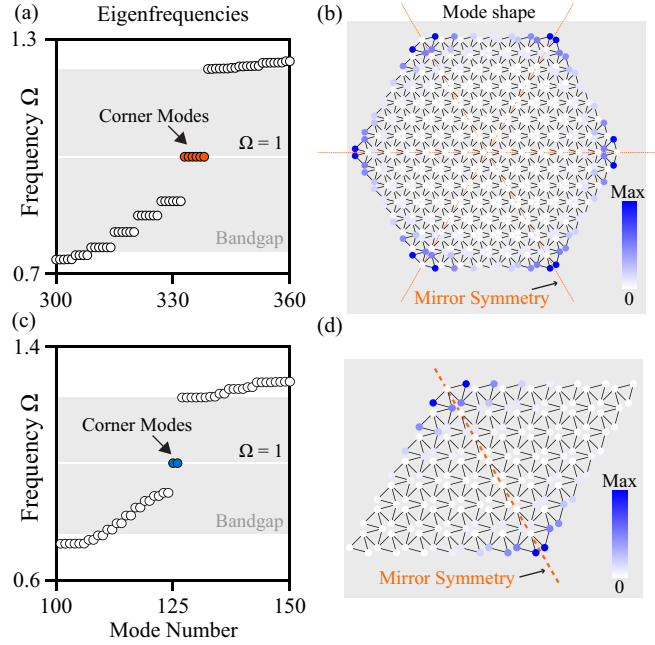

FIG. 2. (a) Eigenfrequency solutions for a finite hexagon-shaped self-dual kagome lattice with six corner modes at an in-gap frequency of $\Omega = 1$ and (b) the mode shape for the corresponding in-gap corner modes localized at the corners of a hexagon. (c) Eigenfrequency solutions for a finite parallelogram-shaped self-dual kagome lattice with two corner modes at an in-gap frequency of $\Omega = 1$ and (d) the mode shape for the two in-gap corner modes localized at the two corners of a parallelogram which lie on a mirror symmetry plane.

transition of a deformed kagome lattice with uniform soft twisting and the resulting transformations in floppy edge modes. Recently, the continuum approach has been applied to explain the elastic behavior of twisted kagome lattices for zero-frequency modes [49] and topological edge soft modes in topological kagome lattices [50]. More recently, Gonella [51] elucidated the dual nature of the twisted kagome lattice, originally put forward by Fruchart *et al.* [43], using bidomain lattice structures and demonstrated the dependence of the duality behavior on the underlying mechanism of cell deformation. On the other hand, following the work of Xue *et al.* [37] on an acoustic higher-order topological insulator on a kagome lattice, Wu *et al.* [52] experimentally observed second-order topologically protected corner states in a regular elastic kagome lattice. While rich in dynamics, studies of the corner modes in elastic twisted kagome lattices are lacking. It is therefore the aim of this study to demonstrate the existence of corner modes in a twisted kagome lattice and to explain their relationship to structural symmetries and bulk polarization, as well as to propound the necessary conditions for their manifestation. To this end, we also explore the analogous electronic system to explain the existence of corner modes via bulk polarization and Wannier centers.

We first demonstrate the emergence of corner modes considering a finite self-dual kagome lattice having a shape of a regular hexagon. The self-dual kagome lattice has three mirror symmetry planes oriented at angles 0, $\pi/3$, and $2\pi/3$ (measured counterclockwise from a horizontal line), which pass through the corners of the hexagonal structure. We choose a hexagon lattice size of seven unit cells on each edge, which is sufficiently large to observe the in-gap corner eigenfrequencies, as shown in Fig. 2(a). There exist six corner modes (one for each corner) at an in-gap frequency of $\Omega = \omega\sqrt{\frac{m}{k}} = 1$. The mode shape obtained by a linear combination of six eigenmodes at $\Omega = 1$ is depicted in Fig. 2(b). It shows highly localized deformation at the six corners of the hexagonal structure. Interestingly, the mode shapes corresponding to the corner modes show zero deformation of the lattice site lying on the mirror symmetry planes, a behavior that extends to all lattice sites of the same type in the vicinity of the corner. Other modes appearing in the band gap [Fig. 2(a)] are edge modes localized around the edges of the hexagon, which appear in pairs due to the duality symmetry.

The appearance of corner modes at $\Omega = 1$, in fact, depends on the shape of the corner and the plane of symmetry. To demonstrate this dependence, consider a finite structure with an overall shape of a parallelogram, which only has a single mirror symmetry plane. While the structure has four total corners, only two corner modes appear at $\Omega = 1$ in the eigenfrequency calculations as depicted in Fig. 2(c). As anticipated, the mode shapes of these corner modes are localized at the corners located at the symmetry planes as shown in Fig. 2(d). This example emphasizes the importance of the existence of mirror symmetry for the manifestation of corner modes. An intriguing observation from both analyzed finite structures is that the corner modes always appear at a normalized frequency of $\Omega = 1$.

The corner modes described above are specific to the self-dual point. The finite hexagon- and parallelogram-shaped lattices away from the self-dual point show corner modes appearing at different frequencies below and above the frequency $\Omega = 1$. For instance, the eigenfrequencies of the corner modes for a finite hexagon-shaped lattice along with the mode shapes for twist angles $\theta = 35^\circ$ and $\theta = 55^\circ$ are shown in Figs. 3(a) and 3(b), respectively. The eigenfrequencies for the two configurations are exactly identical because of the duality and the corner modes appear in groups of three, one group at $\Omega = 0.976$ and the other group at $\Omega = 1.035$. The set of corners localized at the same frequency is of a similar nature, as can be seen from the lattice geometry.

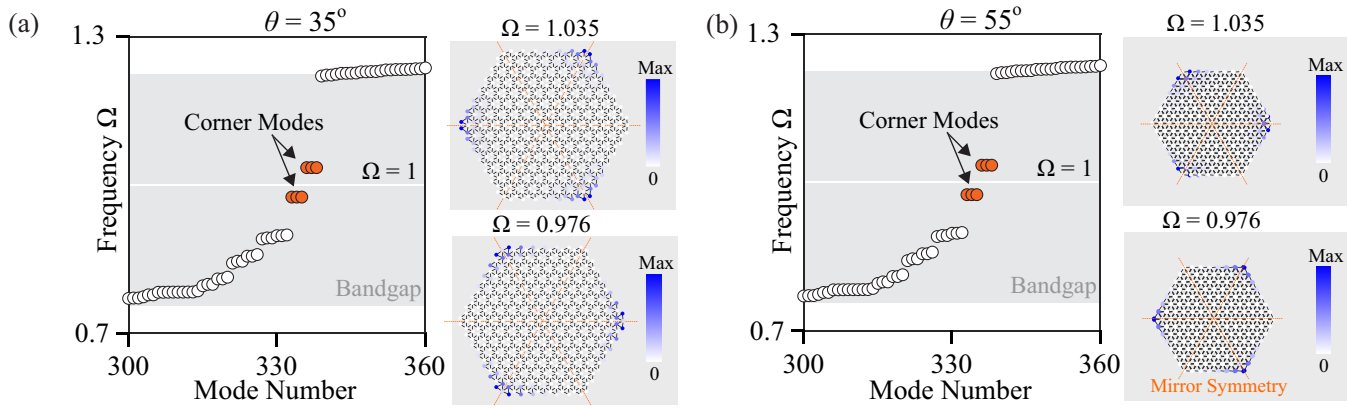

FIG. 3. Eigenfrequency solutions and mode shapes of the corner modes of a finite hexagon-shaped twisted kagome lattice for twist angles (a) $\theta = 35^\circ$ and (b) $\theta = 55^\circ$. Note that the kagome lattice shrinks with increasing twist angle as the two triangles in the unit cell come closer to each other; hence, the hexagonal lattice at $\theta = 55^\circ$ is smaller than the hexagonal lattice at $\theta = 35^\circ$.

Interestingly, the frequency at which the localization happens at a particular set of corners switches to the other corner mode frequency while going from one configuration of the dual lattice pair to the other. For example, the localized set of corners at $\Omega = 0.976$ for $\theta = 35^\circ$ is similar to the localized set of corners at $\Omega = 1.035$ for $\theta = 55^\circ$. The transition occurs about the self-dual point where all six corners are localized at a single frequency of $\Omega = 1$. Furthermore, the deformation of the lattice site of corner unit cells lying on mirror symmetry planes is not zero for the corner modes appearing at twist angles $\theta = 35^\circ$ and $\theta = 55^\circ$ which happens to be a characteristic feature at the self-dual point only.

Next, we investigate the emergence of edge and corner modes by drawing analogies to electronic topological insulators [53–59]. Electronic lattices can be described by a tight-binding Hamiltonian $H(\mathbf{k})$, which is a matrix in momentum space (k space) consisting of electronic hopping and on-site potential terms. By analyzing the topological properties of $H(\mathbf{k})$, we can determine whether there are electronic eigenstates of the Hamiltonian that are localized at the edges or corners of the crystal. Similar techniques can also be applied to the dynamical matrix $D(\mathbf{k})$ in the elastic system. If corner or edge modes exist for the electronic system whose Hamiltonian $H(\mathbf{k})$ has the same matrix form as $D(\mathbf{k})$, then these modes also exist for the corresponding elastic system.

The existence of corner or edge modes in electronic systems can be examined by computing the Wannier centers [58], which represent the center of the electric charge inside the unit cells for each band. Wannier centers are determined by the wave functions in each band, and the total electric polarization can be obtained by summing Wannier centers over all the occupied bands. In the presence of crystalline symmetries, the Wannier centers may be pinned to some specific high-symmetry locations inside each unit cell called Wyckoff positions. For example, in a simple one-dimensional (1D) lattice with one electron in each unit cell as in Fig. 4, if the lattice has mirror symmetry, then the Wannier centers can only be at the Wyckoff position $1a$ at the center or $1b$ at the boundary of each unit cell so that the mirror symmetry is preserved. In Fig. 4(a), there is no edge mode. In Fig. 4(b), edge modes appear because the Wannier center is at the boundary of each unit cell. In Fig. 4(c), edge modes also appear because the edge of the lattice does not have a complete unit cell, although the Wannier centers are at the center of each unit cell in the bulk.

To study the corner modes in a twisted kagome lattice, consider the hexagon-shaped lattice setup in Fig. 5(a) in which all the bonds have the same spring constant. We can treat the dynamical matrix in momentum (k) space as the Hamiltonian for some electronic systems. This system has crystalline symmetry $p31m$ (wallpaper group 15) in addition to time-reversal and duality symmetries. We choose the unit cell to be the blue hexagon in Fig. 5(a) which preserves threefold rotation C_3 and all the mirror symmetries. We next consider the electron polarization for the lowest two bands. C_3 symmetry quantizes the polarization to be $\mathbf{P} = ep(\mathbf{a}_1 + \mathbf{a}_2)$, where e is the electron charge, $\mathbf{a}_1$ and $\mathbf{a}_2$ are direct lattice primitive vectors (see Fig. 1), and $p = 0, 1/3, 2/3$ corresponds to Wyckoff positions $1a$ or $2b$ [58]. However, the $2b$ position is not invariant under mirror symmetry, therefore, with both C_3 and mirror symmetry, the polarization must vanish. For the two lowest bands to have vanishing total polarization, their Wannier centers may either both locate at the $1a$ position, or at the two distinct $2b$ positions. This can be further distinguished by analyzing the symmetry representations of the two lowest bands at high-symmetry momenta (Γ, K, and M in Fig. 1) [53].

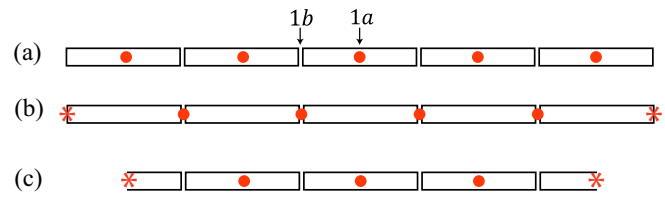

FIG. 4. (a) One-dimensional lattice with mirror reflection symmetry. The unit cells are denoted by black boxes. Wannier centers are represented by red circles. Depending on the form of wave functions, Wannier centers may locate at different Wyckoff positions $1a$ or $1b$. Edge modes appear in (b) and (c) in which the Wannier centers appear at the edge of the crystal, as indicated by the red stars.

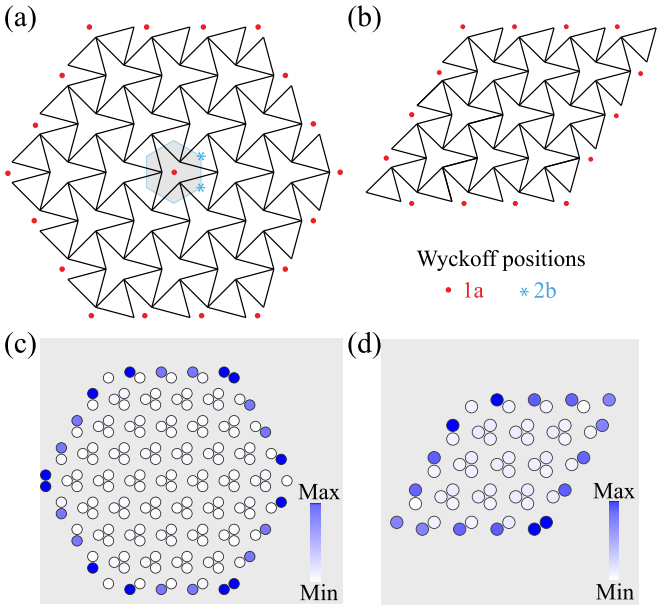

FIG. 5. (a) Hexagon-shaped lattice setup with all springs having the same spring constant. The unit cell is chosen to be the blue hexagon which preserves all crystalline symmetry. Wyckoff positions $1a$ and $2b$ are labeled as red dots and blue stars, respectively. The exposed $1a$ positions at the boundary lead to edge and corner modes. (b) For the parallelogram lattice setup, the 60° corner does not have exposed $1a$ positions, and the corner modes only appear at the 120° corners, as shown in Fig. 2. Charge accumulation at the edges and corners of (c) hexagon-shaped and (d) parallelogram-shaped lattices.

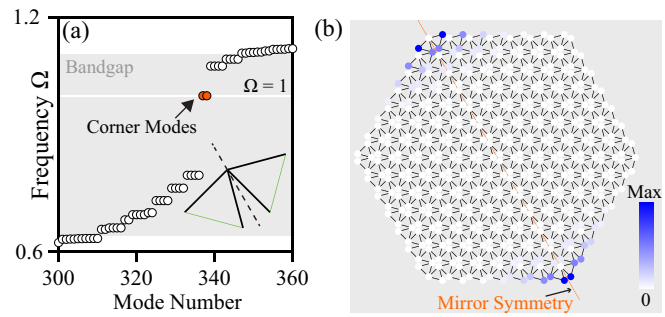

FIG. 6. (a) Eigenfrequencies of a perturbed hexagon-shaped lattice self-dual kagome lattice, where the stiffness of thin (green) links, as depicted in the inset, is made half of the original value (black links). (b) Mode shape of the corner modes at $\Omega = 1$, where the localization of the modes is at the corners which are on the mirror plane, and the number of mirror symmetry planes in the lattice reduces from 3 to 1 because of the perturbation.

In the presence of symmetries, wave functions at each high-symmetry momentum point (Γ, K, and M) will transform as irreducible representations (irreps) of the symmetry group at that momentum point (little group). The high-symmetry momentum Γ, K, and $-K$ are invariant under threefold rotation C_3 and the three mirror symmetries (up to a shift by some reciprocal lattice vector), and their little group is C_{3v}. The high-symmetry momentum M is invariant only under one of the mirror symmetries, and the little group is C_s. The Wannier centers are determined by the irreps of wave functions at these high-symmetry momenta. In particular, if the Wannier centers for the two lowest bands are both at the $1a$ position, then the irreps at Γ and K should be the irrep E of group C_{3v}, and the wave functions at M should have mirror eigenvalues ± 1. We can explicitly check the irreps at each high-symmetry momentum by examining the eigenstates of the dynamical matrix. The dynamical matrix $D(\mathbf{k})$ in momentum space is computed in the SM. A direct computation of the irreps at the high-symmetry momentum points confirms that the irreps at Γ and K are indeed E and the Wannier centers of the two lowest bands are at the $1a$ position.

The existence of edge and corner modes can be inferred from the Wannier centers. If the whole lattice has an integer number of unit cells, there will be no charge accumulation at the boundary because the Wannier centers are at $1a$ inside each unit cell, similar to the scenario in Fig. 4(a). However, the finite lattice in Fig. 5(a) has incomplete unit cells whose Wannier centers at $1a$ are exposed at the boundary, i.e., the red dots. These exposed Wannier centers lead to modes localized at the edges and corners, similar to Fig. 4(c). For the parallelogram setup in Fig. 5(b), since there is no exposed $1a$ position at the 60° corners, the corner modes only exist at the 120° corners. Note that although the corner modes here are reminiscent of those in higher-order topological insulators, the corner charge is not well defined because of the nonzero edge charge. In this system, the bulk polarization measured in a symmetric unit cell [the hexagon in Fig. 5(a)] is zero, and according to Ref. [58] it should not have edge polarization if the boundary contains complete unit cells. However, the boundary termination of the twisted kagome lattice is incommensurate with the symmetric hexagon unit cell. This leads to incomplete unit cells at the boundary as in Figs. 5(a) and 4(c), which is beyond Ref. [58] where complete unit cells at the boundary are assumed. Therefore, the edge and corner modes still emerge due to the incommensurate boundary termination although the bulk polarization vanishes. This is an example of termination-induced boundary modes.

The electronic charge distribution depicting the charge accumulation at the corners and sides of the hexagon and parallelogram are as shown in Figs. 5(c) and 5(d), respectively. The density is obtained at each lattice site by summing the squared norm of eigenvectors up to the corner modes at frequency $\Omega = 1$. The charge density is highest at the lattice sites of unit cells which form the 120° angled corners. The charge accumulated on the edges of the finite lattice is because of the edge modes in the band gap. The charge accumulation corresponds to a high quantum wave amplitude and by analogy the mechanical corner modes have a high elastic wave amplitude at the corner unit cells.

Finally, we show an example of obtaining corner modes at specific corners by carefully perturbing the unit cell links. For the hexagonal structure analyzed in Fig. 2, we choose to reduce the stiffness of two links by a factor of $1/2$ [depicted by thin (green) lines in the inset of Fig. 6(a)], such that a single mirror symmetry plane is retained. Interestingly, the dispersion relation of the perturbed lattice preserve the degeneracy of the bands as well as duality, i.e., identical dispersion characteristics for lattices with twist angles equidistant from the self-dual point. Note that the frequency $\Omega = 1$ is still in the

first band gap of the perturbed lattice. We construct a similar hexagonal finite lattice as in Fig. 2, yet with perturbed links, the eigenfrequency solutions for which are shown in Fig. 6(a). In this case, only two corner modes are observed at $\Omega = 1$ and they are localized around the corners of the hexagon, which lie on the sole mirror symmetry plane of the perturbed lattice. Once again, the mode shape shown in Fig. 6(b) is characterized by zero deformation of the lattice site in the corner unit cells, which lie on a mirror symmetry plane.

The corner modes observed in twisted kagome lattices are reminiscent of the second-order topologically protected states in acoustic [37] and elastic [52] regular kagome lattices which rely on nontrivial bulk topology characterized by quantized Wannier centers. The corner modes observed in these studies are also shape dependent and appear only at the corners with specific angles formed by the edges which cut through the Wannier centers. Despite these similarities, the origin of the edge and corner modes in twisted kagome lattices is distinct from the other systems. In twisted kagome lattices, C_3 and mirror symmetries quantize the Wannier centers to Wyckoff position $1a$, leading to a vanishing bulk polarization. The edge and corner modes emerge due to the incompatibility between the lattice termination and bulk unit cell, even though the bulk of the system is a trivial atomic limit with vanishing polarization. The corner modes are found to be robust to any defects in the bulk (see Supplemental Material for more details [44]).

In summary, we demonstrated the emergence of corner modes in a self-dual kagome lattice that appear at certain corners. Such corner modes were explained in light of an analogy to electronic insulators, which shows these boundary modes are induced by the lattice termination that is incompatible with the bulk unit cell. The robustness of the self-dual kagome lattices and their reconfigurable wave localization at specific corners may find different approaches in various applications such as sensing and energy harvesting.

The authors extend their thanks to Dr. Kai Sun for fruitful discussions on corner modes and Maxwell lattices.

[1] M. Sigalas and E. Economou, Band structure of elastic waves in two dimensional systems, Solid State Commun. **86**, 141 (1993).
[2] M. S. Kushwaha, P. Halevi, L. Dobrzynski, and B. Djafari-Rouhani, Acoustic Band Structure of Periodic Elastic Composites, Phys. Rev. Lett. **71**, 2022 (1993).
[3] R. Martínez-Sala, J. Sancho, J. V. Sánchez, V. Gómez, J. Llinares, and F. Meseguer, Sound attenuation by sculpture, Nature (London) **378**, 241 (1995).
[4] M. Born and K. Huang, Dynamical theory of crystal lattices, Am. J. Phys. **23**, 474 (1955).
[5] K. M. Leung and Y. F. Liu, Full Vector Wave Calculation of Photonic Band Structures in Face-Centered-Cubic Dielectric Media, Phys. Rev. Lett. **65**, 2646 (1990).
[6] Z. Zhang and S. Satpathy, Electromagnetic Wave Propagation in Periodic Structures: Bloch Wave Solution of Maxwell's Equations, Phys. Rev. Lett. **65**, 2650 (1990).
[7] K. M. Ho, C. T. Chan, and C. M. Soukoulis, Existence of a Photonic Gap in Periodic Dielectric Structures, Phys. Rev. Lett. **65**, 3152 (1990).
[8] J. H. Page, P. Sheng, H. P. Schriemer, I. Jones, X. Jing, and D. A. Weitz, Group velocity in strongly scattering media, Science **271**, 634 (1996).
[9] P. Deymier, *Acoustic Metamaterials and Phononic Crystals* (Springer, Berlin, 2013).
[10] V. Laude, *Phononic Crystals* (de Gruyter, Berlin, 2015).
[11] C. Goffaux, F. Maseri, J. O. Vasseur, B. Djafari-Rouhani, and P. Lambin, Measurements and calculations of the sound attenuation by a phononic band gap structure suitable for an insulating partition application, Appl. Phys. Lett. **83**, 281 (2003).
[12] Z. Lin, H. B. Al Ba'ba'a, and S. Tol, Piezoelectric metastructures for simultaneous broadband energy harvesting and vibration suppression of traveling waves, Smart Mater. Struct. **30**, 075037 (2021).
[13] M. Farhat, S. Guenneau, and S. Enoch, Ultrabroadband Elastic Cloaking in Thin Plates, Phys. Rev. Lett. **103**, 024301 (2009).
[14] Y. Jin, B. Djafari-Rouhani, and D. Torrent, Gradient index phononic crystals and metamaterials, Nanophotonics **8**, 685 (2019).
[15] H. Danawe, G. Okudan, D. Ozevin, and S. Tol, Conformal gradient-index phononic crystal lens for ultrasonic wave focusing in pipe-like structures, Appl. Phys. Lett. **117**, 021906 (2020).
[16] A. Sukhovich, L. Jing, and J. H. Page, Negative refraction and focusing of ultrasound in two-dimensional phononic crystals, Phys. Rev. B **77**, 014301 (2008).
[17] S. Tol, F. Degertekin, and A. Erturk, 3D-printed phononic crystal lens for elastic wave focusing and energy harvesting, Addit. Manuf. **29**, 100780 (2019).
[18] G. Ma, M. Xiao, and C. T. Chan, Topological phases in acoustic and mechanical systems, Nat. Rev. Phys. **1**, 281 (2019).
[19] X. Ni, M. A. Gorlach, A. Alu, and A. B. Khanikaev, Topological edge states in acoustic kagome lattices, New J. Phys. **19**, 055002 (2017).
[20] H. Chen, H. Nassar, and G. L. Huang, A study of topological effects in 1D and 2D mechanical lattices, J. Mech. Phys. Solids **117**, 22 (2018).
[21] R. Süsstrunk and S. D. Huber, Classification of topological phonons in linear mechanical metamaterials, Proc. Natl. Acad. Sci. USA **113**, E4767 (2016).
[22] X. Zhang, M. Xiao, Y. Cheng, M.-H. Lu, and J. Christensen, Topological sound, Commun. Phys. **1**, 97 (2018).
[23] P. Wang, L. Lu, and K. Bertoldi, Topological Phononic Crystals with One-Way Elastic Edge Waves, Phys. Rev. Lett. **115**, 104302 (2015).
[24] H. Chen, L. Y. Yao, H. Nassar, and G. L. Huang, Mechanical Quantum Hall Effect in Time-Modulated Elastic Materials, Phys. Rev. Appl. **11**, 044029 (2019).
[25] L. M. Nash, D. Kleckner, A. Read, V. Vitelli, A. M. Turner, and W. T. Irvine, Topological mechanics of gyroscopic metamaterials, Proc. Natl. Acad. Sci. USA **112**, 14495 (2015).
[26] R. Chaunsali, C. W. Chen, and J. Yang, Experimental demonstration of topological waveguiding in elastic plates with local resonators, New J. Phys. **20**, 113036 (2018).
[27] H. Chen, H. Nassar, A. N. Norris, G. K. Hu, and G. L. Huang, Elastic quantum spin Hall effect in kagome lattices, Phys. Rev. B **98**, 094302 (2018).

[28] Y. Chen, X. Liu, and G. Hu, Topological phase transition in mechanical honeycomb lattice, J. Mech. Phys. Solids **122**, 54 (2019).

[29] R. K. Pal and M. Ruzzene, Edge waves in plates with resonators: An elastic analogue of the quantum valley Hall effect, New J. Phys. **19**, 25001 (2017).

[30] H. Al Ba'ba'a, K. Yu, and Q. Wang, Elastically-supported lattices for tunable mechanical topological insulators, Extreme Mech. Lett. **38**, 100758 (2020).

[31] T. W. Liu and F. Semperlotti, Experimental Evidence of Robust Acoustic Valley Hall Edge States in a Nonresonant Topological Elastic Waveguide, Phys. Rev. Appl. **11**, 014040 (2019).

[32] E. Prodan, K. Dobiszewski, A. Kanwal, J. Palmieri, and C. Prodan, Dynamical Majorana edge modes in a broad class of topological mechanical systems, Nat. Commun. **8**, 14587 (2017).

[33] H. Al Ba'ba'a, M. Nouh, and T. Singh, Dispersion and topological characteristics of permutative polyatomic phononic crystals, Proc. R. Soc. A **475**, 20190022 (2019).

[34] M. I. N. Rosa, R. K. Pal, J. R. F. Arruda, and M. Ruzzene, Edge States and Topological Pumping in Spatially Modulated Elastic Lattices, Phys. Rev. Lett. **123**, 034301 (2019).

[35] E. Riva, M. I. N. Rosa, and M. Ruzzene, Edge states and topological pumping in stiffness-modulated elastic plates, Phys. Rev. B **101**, 094307 (2020).

[36] M. Serra-Garcia, V. Peri, R. Süsstrunk, O. R. Bilal, T. Larsen, L. G. Villanueva, and S. D. Huber, Observation of a phononic quadrupole topological insulator, Nature (London) **555**, 342 (2018).

[37] H. Xue, Y. Yang, F. Gao, Y. Chong, and B. Zhang, Acoustic higher-order topological insulator on a kagome lattice, Nat. Mater. **18**, 108 (2019).

[38] H. Fan, B. Xia, L. Tong, S. Zheng, and D. Yu, Elastic Higher-Order Topological Insulator with Topologically Protected Corner States, Phys. Rev. Lett. **122**, 204301 (2019).

[39] X. Mao and T. C. Lubensky, Maxwell lattices and topological mechanics, Annu. Rev. Condens. Matter Phys. **9**, 413 (2018).

[40] L. Zhang and X. Mao, Fracturing of topological Maxwell lattices, New J. Phys. **20**, 063034 (2018).

[41] D. Zhou, J. Ma, K. Sun, S. Gonella, and X. Mao, Switchable phonon diodes using nonlinear topological Maxwell lattices, Phys. Rev. B **101**, 104106 (2020).

[42] T. Lubensky, C. Kane, X. Mao, A. Souslov, and K. Sun, Phonons and elasticity in critically coordinated lattices, Rep. Prog. Phys. **78**, 073901 (2015).

[43] M. Fruchart, Y. Zhou, and V. Vitelli, Dualities and non-Abelian mechanics, Nature (London) **577**, 636 (2020).

[44] See Supplemental Material at http://link.aps.org/supplemental/10.1103/PhysRevB.104.L241107 for more details on the analytical formulation and dispersion curve calculations of a mechanical twisted kagome lattice and the robustness of the corner modes at the self-dual point.

[45] M. I. Hussein, M. J. Leamy, and M. Ruzzene, Dynamics of phononic materials and structures: Historical origins, recent progress, and future outlook, Appl. Mech. Rev **66**, 040802 (2014).

[46] R. Hutchinson and N. Fleck, The structural performance of the periodic truss, J. Mech. Phys. Solids **54**, 756 (2006).

[47] K. Sun, A. Souslov, X. Mao, and T. C. Lubensky, Surface phonons, elastic response, and conformal invariance in twisted kagome lattices, Proc. Natl. Acad. Sci. USA **109**, 12369 (2012).

[48] D. Rocklin, S. Zhou, K. Sun, and X. Mao, Transformable topological mechanical metamaterials, Nat. Commun. **8**, 14201 (2017).

[49] H. Nassar, H. Chen, and G. Huang, Microtwist elasticity: A continuum approach to zero modes and topological polarization in kagome lattices, J. Mech. Phys. Solids **144**, 104107 (2020).

[50] K. Sun and X. Mao, Continuum Theory for Topological Edge Soft Modes, Phys. Rev. Lett. **124**, 207601 (2020).

[51] S. Gonella, Symmetry of the phononic landscape of twisted kagome lattices across the duality boundary, Phys. Rev. B **102**, 140301(R) (2020).

[52] Q. Wu, H. Chen, X. Li, and G. Huang, In-Plane Second-Order Topologically Protected States in Elastic Kagome Lattices, Phys. Rev. Applied **14**, 014084 (2020).

[53] B. Bradlyn, L. Elcoro, J. Cano, M. G. Vergniory, Z. Wang, C. Felser, M. I. Aroyo, and B. A. Bernevig, Topological quantum chemistry, Nature (London) **547**, 298 (2017).

[54] H. C. Po, A. Vishwanath, and H. Watanabe, Symmetry-based indicators of band topology in the 230 space groups, Nat. Commun. **8**, 50 (2017).

[55] W. A. Benalcazar, B. A. Bernevig, and T. L. Hughes, Quantized electric multipole insulators, Science **357**, 61 (2017).

[56] W. A. Benalcazar, B. A. Bernevig, and T. L. Hughes, Electric multipole moments, topological multipole moment pumping, and chiral hinge states in crystalline insulators, Phys. Rev. B **96**, 245115 (2017).

[57] F. Schindler, A. M. Cook, M. G. Vergniory, Z. Wang, S. S. P. Parkin, B. A. Bernevig, and T. Neupert, Higher-order topological insulators, Sci. Adv **4**, eaat0346 (2018).

[58] W. A. Benalcazar, T. Li, and T. L. Hughes, Quantization of fractional corner charge in C_n-symmetric higher-order topological crystalline insulators, Phys. Rev. B **99**, 245151 (2019).

[59] Z. Song, Z. Fang, and C. Fang, $(d-2)$-Dimensional Edge States of Rotation Symmetry Protected Topological States, Phys. Rev. Lett. **119**, 246402 (2017).